infrastructures

MDPI

Article

Jointed Plain Concrete Pavements in Airports: Structural–Economic Evaluation and Proposal for a Catalogue

Paola Di Mascio [1], Alberto De Rubeis [2], Claudio De Marchis [3], Antonello Germinario [3], Giovanni Metta [4], Rosario Salzillo [4] and Laura Moretti [1,*]

1 Department of Civil, Constructional and Environmental Engineering, Sapienza University of Rome, Via Eudossiana 18, 00184 Rome, Italy; paola.dimascio@uniroma1.it
2 Servizio Infrastrutture A.M. (ITAF Infrastructure Department), Viale dell'Università 4, 00185 Rome, Italy; alberto.derubeis@aeronautica.difesa.it
3 Laboratorio Principale Prove e Sperimentazioni, 2° Reparto Genio A.M. (ITAF Infrastructure Department), Viale di Marino snc, 00043 Ciampino, Italy; claudio.demarchis@aeronautica.difesa.it (C.D.M.); antonello.germinario@aeronautica.difesa.it (A.G.)
4 Ufficio Progetti, 2° Reparto Genio A.M. (ITAF Infrastructure Department), Viale di Marino snc, 00043 Ciampino, Italy; giovanni.metta@aeronautica.difesa.it (G.M.); rosario.salzillo@aeronautica.difesa.it (R.S.)
* Correspondence: laura.moretti@uniroma1.it; Tel.: +39-06-44585114

Abstract: Although the design of jointed plain concrete pavements could be solved by commercial software, there is still a need for simple tools to be used in feasibility studies and preliminary cost–benefit analyses. This paper analyzed and verified jointed plain concrete pavements for airports composed of square slabs without tie and dowel bars. The examined slabs are laid on a cement-treated base layer and a stabilized granular subbase layer. The finite element software FAARFIELD was used to design the JPCP pavements when they are subjected to the design of the airplane (i.e., turboprop C-130J Hercules) under different conditions. Seven subgrade load bearing capacity values, twenty traffic levels, and two construction hypotheses (i.e., constant or variable thickness of the two deeper layers) were designed and then verified with the Westergaard theory in order to present a proposal for a catalogue. Finally, the construction cost per unit surface area was calculated for different construction methods of paving (by slip form paver or by fixed form). The obtained results provide a simple and fast procedure to design preliminary airport JPCPs.

Keywords: airport pavement; military airplane; finite element model; concrete pavement; jointed plain concrete pavement

Citation: Di Mascio, P.; De Rubeis, A.; De Marchis, C.; Germinario, A.; Metta, G.; Salzillo, R.; Moretti, L. Jointed Plain Concrete Pavements in Airports: Structural–Economic Evaluation and Proposal for a Catalogue. *Infrastructures* **2021**, *6*, 73. https://doi.org/10.3390/infrastructures6050073

Academic Editors: Fabrizio D'Amico, Luca Bianchini Ciampoli and Fabio Tosti

Received: 8 April 2021
Accepted: 27 April 2021
Published: 11 May 2021

1. Introduction

The first Italian airports were born in the first decades of the last century: they were built for military needs. Those infrastructures were just a large leveled circular area, lawned estate, where airplanes took off or landed in the most favorable wind direction. Over the years, elliptical shapes first and tricuspid hypocycloids then were adopted to minimize the fields' surfaces. Moreover, the increasing aircraft size and weight and the greater demand for resistance to chemical agents (e.g., fuels and anti-freezers) [1] determined the final transition from airfields to paved runways [2]. The Italian Air Force (IAF) designed the first paved runway in 1927 to bear the increasing movements of heavy aircraft. Only in 1938 were paved runways of IAF conceived for operational reasons, in order to guarantee flight operations during rainy periods. Since the Second World War, new airport pavement design methods and construction technologies have been studied to face the dynamic and static stresses induced by aircraft. At present, most of the operative military Italian airports (15) derive from structures built between 1945 and 1975, when the most important changes in performance and payload (e.g., transition from engines to jets) of military aircraft occurred. Runways built during the War or post-War period were composed of concrete slabs on a

granular not crushed base layer. With the transition to jets, these runways were lengthened, widened, and, with the exception of the thresholds, covered with asphalt [3]. Concrete thresholds were resistant to attack by fuel and chemicals, while asphalt ensured regular paved surfaces, without joints [4]. On the other hand, runways built in the 60s and 70s were composed of three bituminous layers on a stabilized subbase, while the thresholds were composed of rigid pavements. Nowadays military runways have flexible or semi-rigid pavements because of their simple building process and low construction costs, while thresholds and parking areas are composed of rigid pavements to prevent rutting and chemical damages [5].

The large experience of the IAF has helped to collect data on design, construction, and maintenance of runways over more than 80 years. With regard to concrete pavements, Jointed Plain Concrete Pavements (JPCP) without dowel and tie bars are the most frequent solution because of simple and rapid execution, lower cost than other concrete solutions (the presence of bars involves an increase in expenditure varying from 8% to 20%, while a continuous reinforcement involves a higher initial expense of 50% or more) [6], good monitored performances [7–11], and simple maintenance works [12,13], the latter with potential applications to other facilities, where regular maintenance might lag behind [14–16]. The absence of reinforcement requires a double foundation layer: a bottom one composed of a granular mixture and a top one composed of a cement-stabilized mixture. Finally, when high traffic volumes are expected, the experience gained with JPCP solution without bars suggests compensating for the absence of bars with a slab thickness increase or with a cement-treated base layer [17].

In the present study, a catalogue of airport pavements is presented. A three-layer pavement is considered (subbase, base, and concrete slab) and two different approaches were followed to design and verify a set of solutions:

1. to keep constant the thickness of the two deeper layers (30 cm for the granular layer and 15 cm for the cement-bound layer) (Figure 1a);
2. to vary the thickness of the bottom layers. This second approach provides three pairs of different thicknesses for the bottom layers as the bearing capacity of the subgrade varies: 50 cm and 25 cm for low bearing capacity, 40 cm and 20 cm for intermediate bearing capacity, and 30 cm and 15 cm for high bearing capacity, for the granular and cement-bound layer, respectively (Figure 1b). This approach aims to evaluate the most convenient pavement given the bearing capacity and the number of movements.

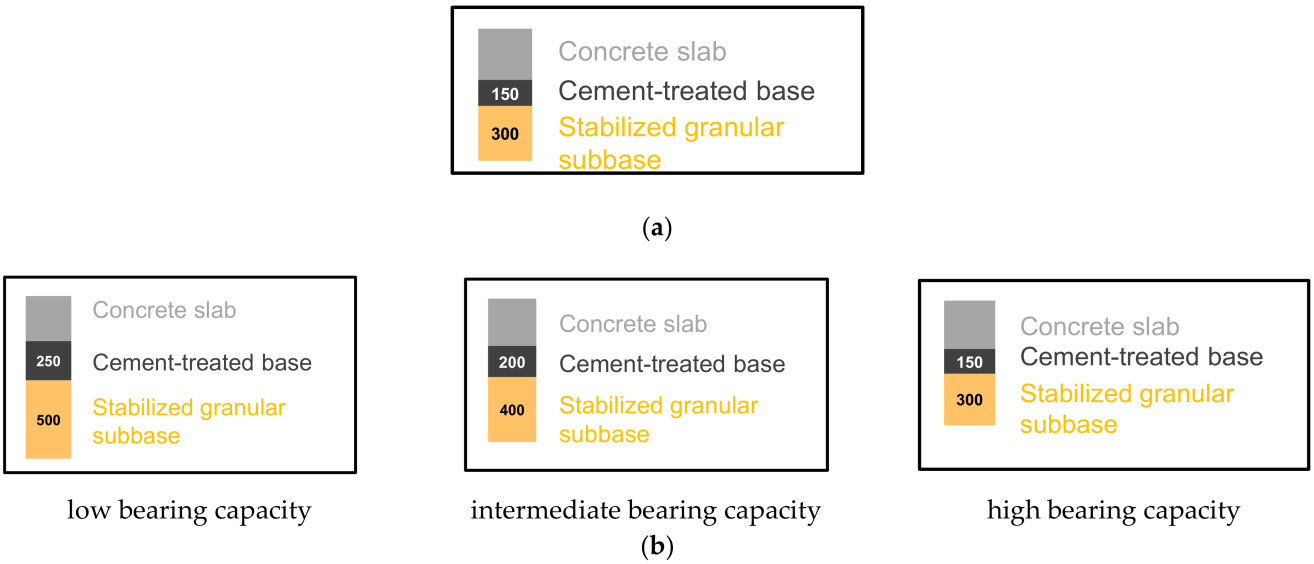

Figure 1. Examined pavements (units: mm). (**a**) Scenario 1; (**b**) scenario 2.

The design of the rigid pavements was carried out with the software FAARFIELD 1.42 (Federal Aviation Administration Rigid and Flexible Iterative Elastic Layered Design) [18]. It exploits the Finite Element Method (FEM) to calculate the stresses and strains and performs the fatigue analysis considering the number of coverages of the design airplane [19]. Each solution was verified by the Westergaard theory [20]. Altogether, the paper proposes several pavement sets to constitute a catalogue considering twenty traffic volumes and seven subgrade load bearing capacity values. Finally, the construction costs of each verified pavement were calculated varying the construction method (i.e., construction by slipform paver or by a fixed form and labor-oriented method of paving). The results of this study answer the need of a faster and easier analysis procedure than the FEM approach that could be used to design block pavements.

2. Data and Methods

In order to analyze a runway pavement, the input data about traffic, reference service life, subgrade load bearing capacity, and performance of materials should be considered [21]. In this study, the reference aircraft is the four-engine turboprop C-130J Hercules (Lockheed Martin, Bethesda, MD, USA), used by the Italian Air Force for civil and military operations (Figure 2). It can operate in 13 of the operative military Italian airports.

Figure 2. C-130J Hercules.

Its load distribution at landing is 5% on the front gear and 95% on the rear one; the other characteristics are listed in Table 1.

Table 1. Technical characteristics of the C-130J.

Characteristic	Value	Unit
Wingspan	40.41	m
Length	29.79	m
Maximum take-off weight	79.38	t
Tire pressure	0.74	MPa
Maximum static load per wheel of the main landing gear	18.8	t

Figure 3 shows the layout of the main landing gears of C-130J: it is a tandem with two single wheels.

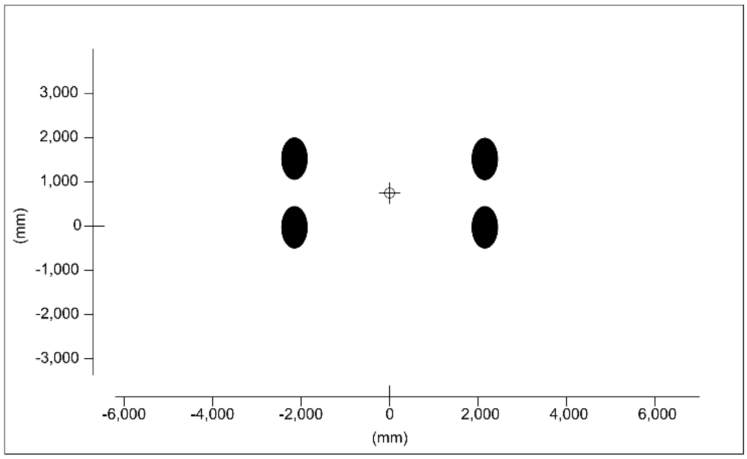

Figure 3. C-130J Hercules.

In this study, the reference service life was 20 years according to the NATO Approved Criteria and Standards for Airfields [22]; 20 traffic levels were considered to define the catalogue: they range between 500 and 10,000 take-offs, in steps of 500.

The load bearing capacity of the subgrade is defined by means of the California Bearing Ratio (CBR) [23] and the equivalent reaction module k is calculated according to Equation (1) [18], where k is in MPa/m.

$$k = 8\ CBR^{0.7788} \quad (1)$$

In this study, CBR varies between 2.5% and 20% (therefore, k ranges between 15.9 and 64.2 MPa/m); this range was divided into 7 sub-intervals of amplitude equal to 2.5%. The lower value of CBR (i.e., 2.5%) is a limit value under which a subgrade stabilization is necessary before building the pavement. The upper value of CBR (i.e., 20%) is assumed as the maximum constant value during the year, when the soil water content varies.

With regard to the materials of the pavement layers, Tables 2–5 list their threshold values and reference standards.

Table 2. Acceptance requirements for granular subbase.

Maximum Diameter (mm)	Variable	Symbol	Standard	Value	Unit
40	Maximum diameter	D_{MAX}	EN 933-2:2020 [24]	40	mm
	Crushed and broken surfaces		EN 933-5:2004 [25]	>90	%
	Resistance to fragmentation		EN 1097-2:2010 [26]	≤40	%
	Shape index		EN 933-4:2008 [27]	≤3	%
	Flakiness index		EN 933-3:2012 [28]	≤20	%
	Freeze/thaw loss		EN 1367-1:2007 [29]	≤30	%
	Passing at 0.0063 mm		EN 933-1 [30]	≤2	%

Table 2. *Cont.*

Maximum Diameter (mm)	Variable	Symbol	Standard	Value	Unit
20	Plasticity index	IP	EN ISO 17892-12:2018 [31]	NP	-
	Liquid limit	W_L	EN ISO 17892-12:2018 [31]	≤25	%
	Sand equivalent	SE	EN 933-8:2015 [32]	≤40	%
	Passing at 0.063 mm		EN 933-2:2020 [24]	≤3	%

Table 3. Gradation limits of granular subbase.

Diameter (mm)	Passing ratio (%)
63	100
31.5	100–45
8	75–32
2	50–15
0.5	34–6
0.063	24–0

Granular stabilized mix should have not less than 80% CBR in the laboratory, performed on samples compliant with [33]. Moreover, the liquid limit W_L should be less than 25%; IP should be equal to zero.

Table 4. Acceptance requirements for aggregates for cement-bound subbase.

Maximum Diameter (mm)	Variable	Symbol	Standard	Value	Unit
40	Maximum diameter	D_{MAX}	EN 933-2:2020 [24]	40	mm
	Crushed and broken surfaces		EN 933-5:2004 [24]	>100	%
	Resistance to fragmentation		EN 1097-2:2010 [26]	≤30	%
	Porosity		EN 1097-2:2010 [26]	≤1.5	%
	Shape index		EN 933-4:2008 [27]	≤1.5	%
	Flakiness index		EN 933-3:2012 [28]	≤20	%
	Freeze/thaw loss		EN 1367-1:2007 [29]	≤30	%
	Passing at 0.063 mm		EN 933-1 [30]	≤2	%
20	Plasticity index	IP	EN ISO 17892-12:2018 [31]	NP-6	-
	Liquid limit	W_L	EN ISO 17892-12:2018 [31]	≤25	%
	Sand equivalent	SE	EN 933-8:2015 [32]	35–25	%
	Passing at 0.063 mm	-	EN 933-2:2020 [24]	≤2	%

Table 5. Gradation limits of aggregates for cement-bound subbase.

Diameter (mm)	Passing Ratio (%)
40	100
31.5	100–80
16	72–47
8	55-30
4	41–21
2	30–24
1	22–10
0.5	15–6
0.250	10–3
0.125	5–1

Cement used in cement-bound subbase should comply with EN 197-1 [34]; water should comply with EN 1008:2002 [35] (Table 6).

Table 6. Mechanical performances of cement-bound subbase.

Parameter	Reference Standard	Value	Unit
Cylindrical characteristic resistance, 7 days	EN 12390-3 [36]	3–7	MPa
Indirect tensile resistance, 7 days	EN 12390-6 [37]	0.45–0.85	MPa

The software FAARFIELD 1.42 was used to design the JPCP pavements: they have a 4-layer structure composed of subgrade, subbase course, base course, and surface course (Figure 4).

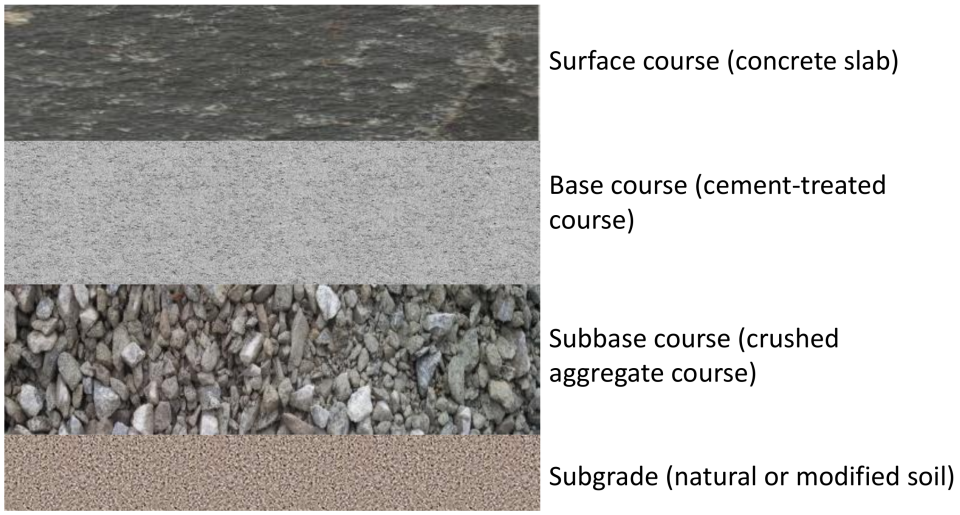

Figure 4. Typical cross section of a JPCP pavement system.

According to AC 150/5370-10G [38], each JPCP layer should satisfy a minimum thickness value for technical reasons (Table 7).

Table 7. Minimum thicknesses.

Layer	Material	Maximum Airplane Gross Weight Operating on Pavement (kg)		
		<5670	<45,360	≥45,360
		Minimum Thickness (mm)		
Surface course	Portland cement concrete	125	150	150
Stabilized base	cement-treated course	not required	not required	125
Base	crushed aggregate	not required	150	150
Subbase	subbase course	100	as needed	as needed

FAARFIELD permits setting of the value of k, the number of years of the service life, and the traffic mix (Figure 5).

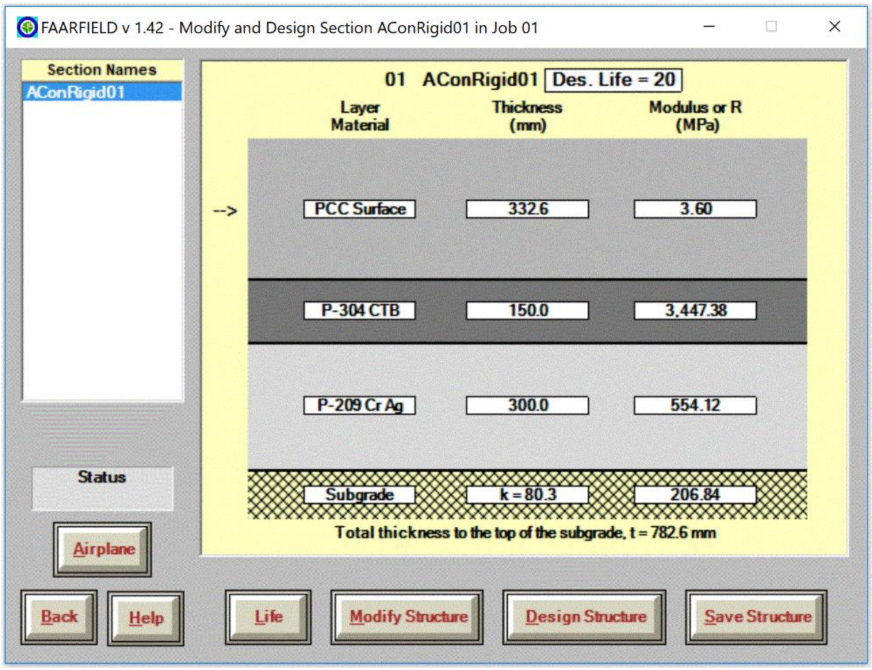

Figure 5. Design section of FAARFIELD.

The value of the Young's modulus of base and subbase layers is automatically set according to the selected materials, while it is possible to define the Modulus of rupture (MOR) of the concrete according to EN 12390-5 [39]. The concrete mix considered in this study is grade C 35/45 [40], with MOR at 28 days not less than 4.1 MPa. Details about concrete mix proportion used for mechanized laying are listed in Table 8.

Table 8. Concrete mix proportion.

Component	Quantity (kg/m^3)
Cement	400
Water	170
Sand	943
Gravel	470
Mixed additive (superplasticizing and air entraining)	3.4

After inputting all the required data, the software provides the thicknesses of the 3 layers over the subgrade. Although not modeled in FAARFIELD 1.42 [18], a geosynthetic

sheet underlay was provided to avoid contamination of the subbase layers with fine material of the subgrade [18]. Finally, the results from FAARFIELD were verified using the Westergaard theory [20]: the maximum tensile stresses at the bottom of the slab for a load at the interior and at the edge of slab or at the top of the slab for a load at the corner were compared to MOR [41]. Finally, construction costs of each catalogued pavement were calculated using national price lists [42], regional price lists [43,44] and price lists provided by experience of the 8th Gruppo Genio Campale. Unit prices were implemented in the VBA code "Economic Sustainability of Concrete pavement" developed by the authors [45]. The initial construction costs of the pavement, including overheads and business profits, were evaluated, while costs for earthworks and subgrade compaction were overlooked. All input variables were compliant with the values adopted by IAF: they were derived from datasets and bills of quantities of realized pavement projects. Three construction methodologies were considered: manual installation with fixed formwork, laying with an owned slipform, and laying with rented an slipform. Manual and mechanized laying differ for the hourly production (10 m^3/h vs. 18 m^3/h, respectively) and for the required labor (9 vs. 5 workers, respectively).

3. Results

Figures 6–9 show the verified JPCP pavements composed of 4 m wide × 4 m long slabs built with a characteristic cube compressive strength (R_{ck}) of concrete equal to 45 MPa (MOR ≥ 4.1 MPa); different input data regarding load bearing capacity and number or repetitions during the service life were considered.

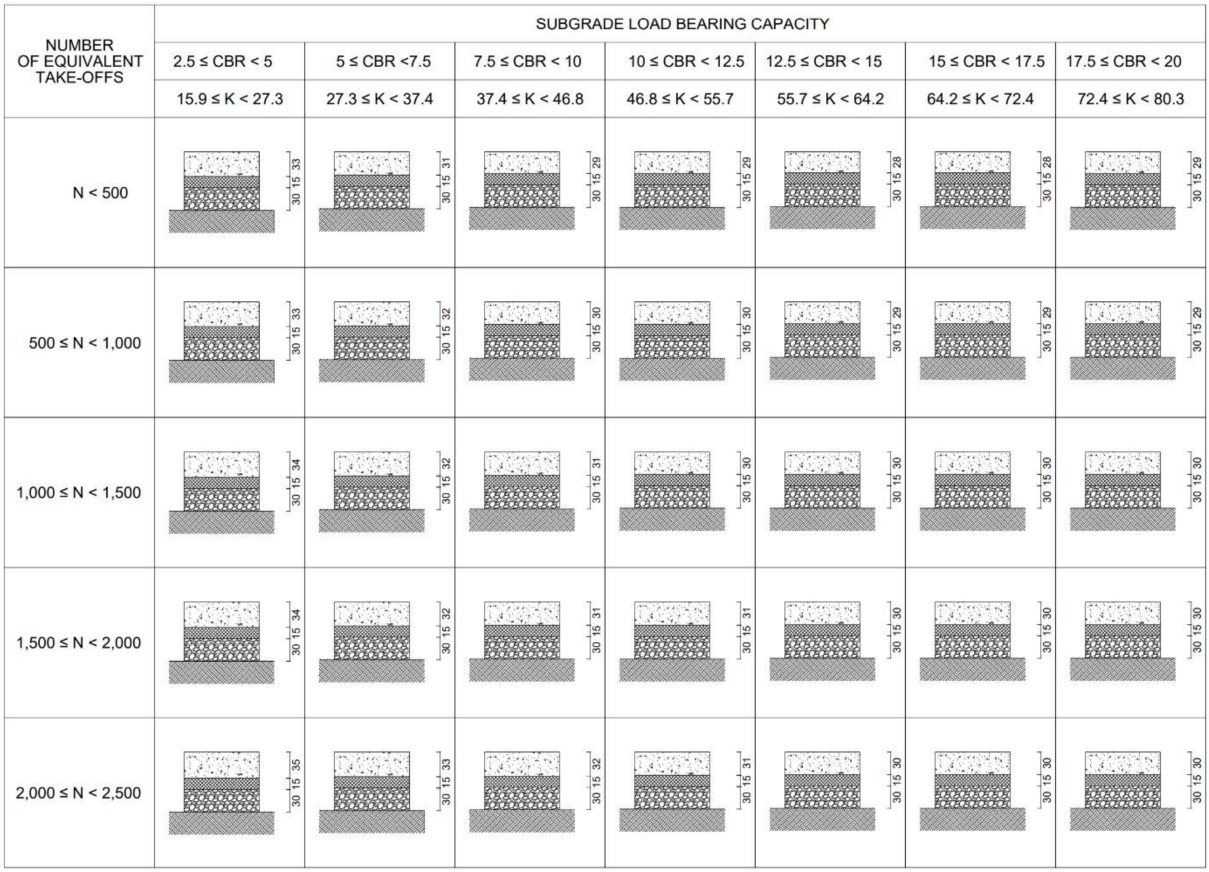

Figure 6. Catalogue of JPCP with a 15 cm-thick cement treated base and 30 cm-thick stabilized subbase (unit: cm); $N < 2000$.

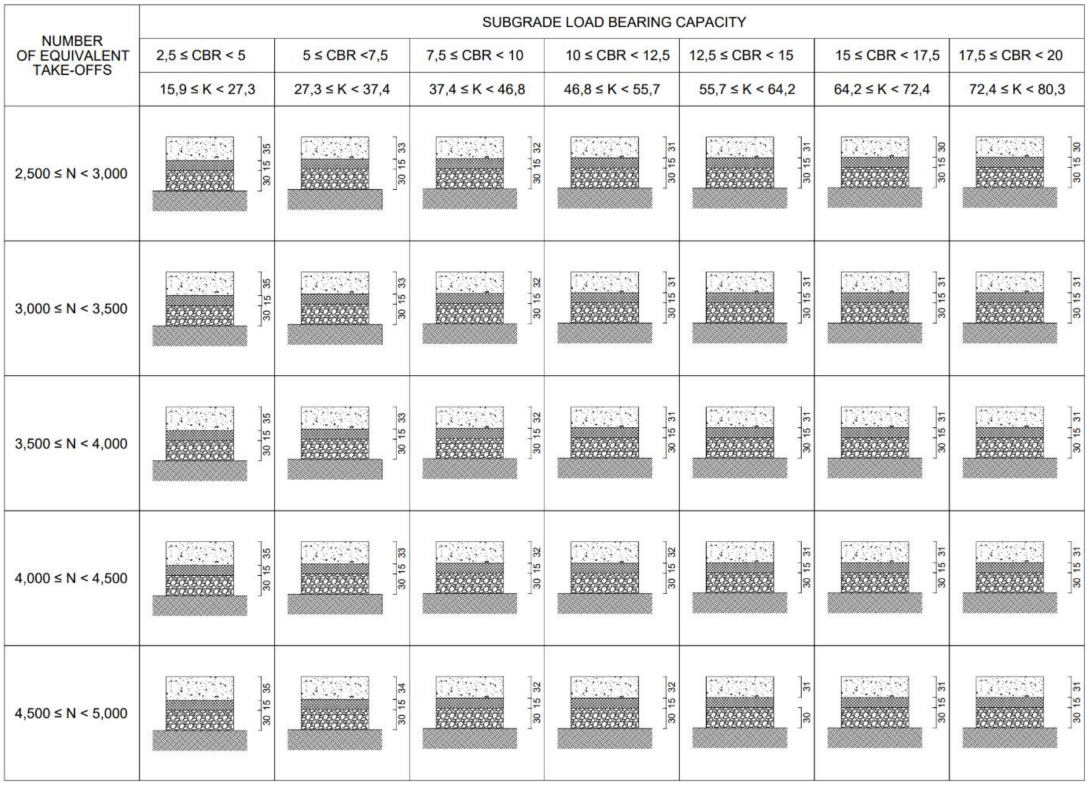

Figure 7. Catalogue of JPCP with a 15 cm-thick cement treated base and 30 cm-thick stabilized subbase (unit: cm); N = 3000–5000.

Data from Figures 6 and 7 permit deepening knowledge of how the subgrade load bearing capacity and the number of movements affect the thickness of the concrete slabs (Table 9) for constant values of MR (i.e., 4.1 MPa) and thickness of the bottom layers (i.e., base and subbase). The cells' color in Table 9 varies from green to red for increasing concrete thickness.

Table 9. Slab thickness for different values of N and CBR—scenario 1.

	Slab Thickness (cm)							
***N* (—)**	**CBR (%)**							
	2.5	**5**	**7.5**	**10**	**12.5**	**15**	**17.5**	**20**
<500	33	31	29	29	28	28	29	29
<1000	33	32	30	30	29	29	29	30
<1500	34	32	31	30	30	30	30	30
<2000	34	32	31	31	30	30	30	30
<2500	35	33	32	31	30	30	30	30
<3000	35	33	32	31	31	30	30	31
<3500	35	33	32	31	31	31	31	31
<4000	35	33	32	31	31	31	31	31
<4500	35	33	32	32	31	31	31	31
<5000	35	34	32	32	31	31	31	31
<5500	35	34	33	32	31	31	31	31
<6000	36	34	33	32	32	31	31	31
<6500	36	34	33	32	32	31	31	31
<7000	36	34	33	32	32	31	31	31
<7500	36	34	33	32	32	32	32	32
<8000	36	34	33	32	32	32	32	32
<8500	36	34	33	32	32	32	32	32
<9000	36	34	33	32	32	32	32	32
<9500	36	34	33	33	32	32	32	32
<10,000	36	34	33	33	32	32	32	32

For a constant value of CBR, the slab thickness increases from 33 cm (*N* equal to 500) to 36 cm (*N* equal to 10,000) for CBR equal to 2.5% and from 29 cm (*N* equal to 500) to 32 cm (*N* equal to 10,000) for CBR equal to 20%. Therefore, the percentage increase in the slab thickness is 9.1% and 10.3%, respectively. For a constant number of repetitions and increasing CBR (from 2.5% to 20%), the percentage decrease in the slab thickness is 9.1% (*N* equal to 500) and 11.1% (*N* equal to 10,000). Since the maximum number of repetitions examined in the study is 20 times more than the minimum one, and the maximum CBR is 8 times more than the minimum one, it is possible to conclude that under the hypotheses of this study the subgrade load bearing capacity affects the slab thickness more than the traffic volume.

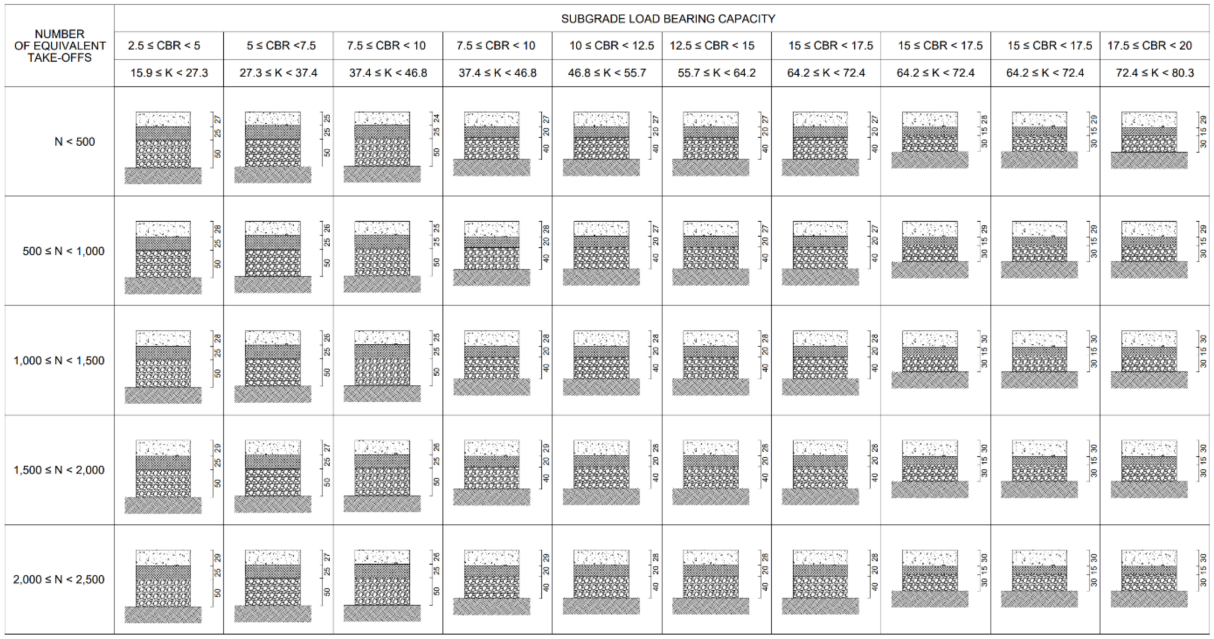

Figure 8. Catalogue of JPCP with variable thickness of the base and subbase (unit: cm); *N* < 2500.

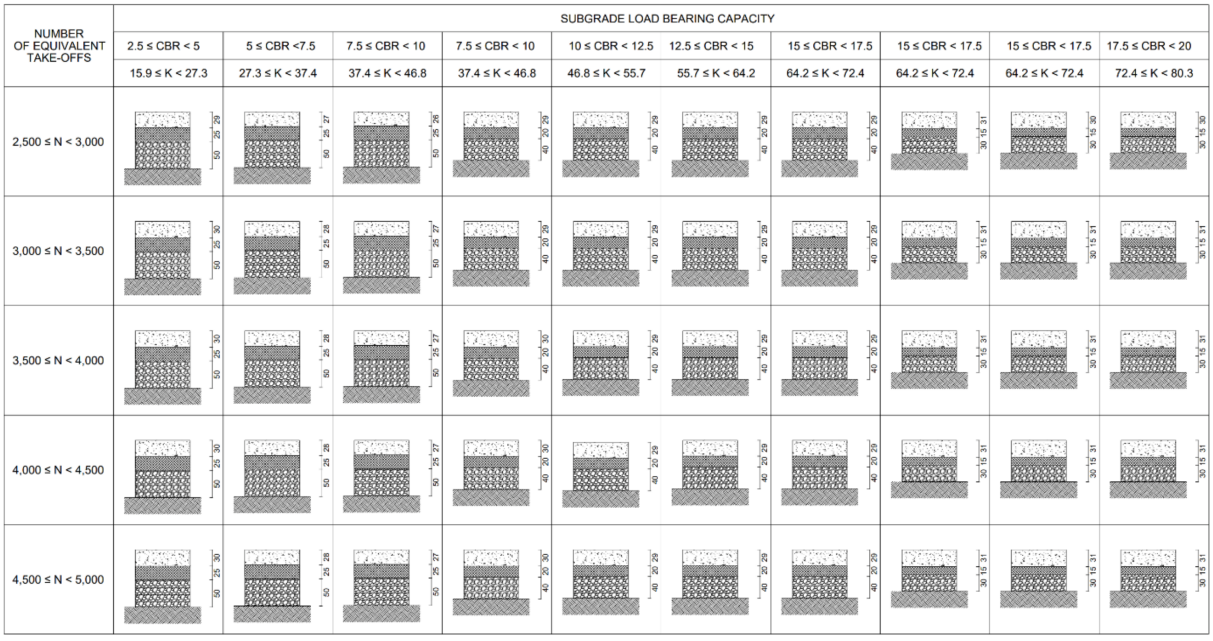

Figure 9. Catalogue of JPCP with variable thickness of the base and subbase (unit: cm); *N* = 2500–5000.

Data from Figures 8 and 9 permit to deepening of knowledge of how the subgrade load bearing capacity and the number of movements affect the thickness of the concrete slabs (Table 10) for constant values of MR (i.e., 4.1 MPa) and variable thickness of the bottom layers (i.e., subbase and base equal to 50 cm and 25 cm for CBR between 2.5% and 10%; 40 cm and 20 cm for CBR between 7.5% and 17.5%; 30 cm and 15 cm for CBR between 15% and 20%). The cells' color in Table 10 complies with that in Table 9.

Table 10. Slab thickness for different values of *N* and CBR—scenario 2.

Slab Thickness (cm)										
N (—)	CBR (%)									
	2.5	5	7.5	7.5	10	12.5	15	15	17.5	20
<500	27	25	24	27	27	27	27	28	29	29
<1000	28	26	25	28	27	27	27	29	29	30
<1500	28	26	25	28	28	28	28	30	30	30
<2000	29	27	26	29	28	28	28	30	30	30
<2500	29	27	26	29	28	28	28	30	30	30
<3000	29	27	26	29	29	29	29	30	30	31
<3500	30	28	27	29	29	29	29	31	31	31
<4000	30	28	27	30	29	29	29	31	31	31
<4500	30	28	27	30	29	29	29	31	31	31
<5000	30	28	27	30	29	29	29	31	31	31
<5500	30	28	27	30	29	29	29	31	31	31
<6000	30	28	27	30	29	29	29	31	31	31
<6500	30	28	27	30	29	29	29	31	31	31
<7000	31	28	27	30	30	29	29	31	31	31
<7500	31	29	28	31	30	29	29	32	32	32
<8000	31	29	28	31	30	30	30	32	32	32
<8500	31	29	28	31	30	30	30	32	32	32
<9000	31	29	28	31	30	30	30	32	32	32
<9500	31	29	28	31	30	30	30	32	32	32
<10,000	31	29	28	31	30	30	30	32	32	32

In Tables 9 and 10, the slab thickness tends to increase against CBR increase for low traffic volumes because the tensile stress under the traffic load depends on the radius of relative stiffness l (Equation (2))

$$l = \sqrt[4]{\frac{Eh^3}{12(1-\nu^2)q}} \tag{2}$$

where E is the Young's modulus of the slab, h is the slab thickness, ν is the Poisson's ratio for concrete, q is the modulus of reaction of the base layer. Since base and subbase layers increase k according to [46], the (constant) maximum allowable load stress according to [20] implies a trend of h that is not monotonous to verify the slab (Equation (3)). Indeed, h affects the tensile stress (σ_C) in the bottom surface of a slab loaded at the interior and away from all the edges:

$$\sigma_c = 0.275 \cdot (1+\nu) \cdot \frac{P}{h^2}\left[4 \cdot \log_{10}\left(\frac{l}{b}\right) + 1.069\right] \tag{3}$$

where P is the applied load and b is the equivalent radius of the resisting section.

The approach of variable thickness of the bottom layer has relevant effects on the slab thickness. For a low subgrade load baring capacity (i.e., CBR between 2.5% and 7.5%), the comparison of the results in Tables 9 and 10 highlights the reduction in the slab thickness for constant N values. In particular, doubling the number of repetitions from 500 to 1000 the percentage increase in the slab thickness is 3.7%, while doubling CBR the percentage decrease in the slab thickness is 7.4%: the base bearing capacity affects the slab thickness more than the traffic volume. This effect is reduced increasing the CBR and reducing

the thickness of the bottom layers (e.g., for CBR between 7.5% and 15% and *N* equal to 500 the slab thickness does not vary, while when doubling *N* it increases from 27 cm to 28 cm). For high CBR values, the trend of slab thickness is opposite to that observed for low CBR values. Therefore, the technical results are needed for the economic analysis of construction costs of the pavements in Figures 6–9 in order to identify the best strategies. In Figures 10–12 the red surface represents costs of the first scenario (i.e., constant thickness of the two deeper layers), while the blue to yellow surface refers to the second scenario (i.e., variable thickness of the bottom layers).

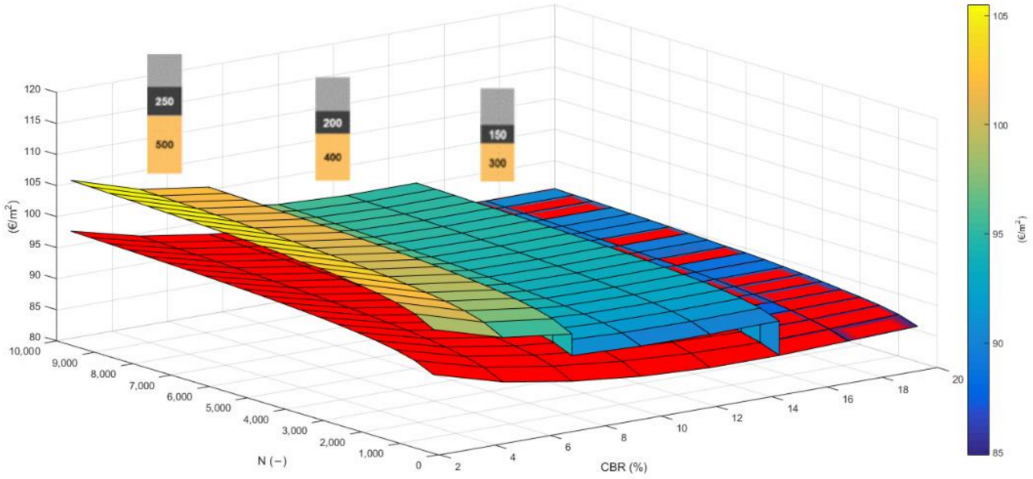

Figure 10. Construction costs with fixed form.

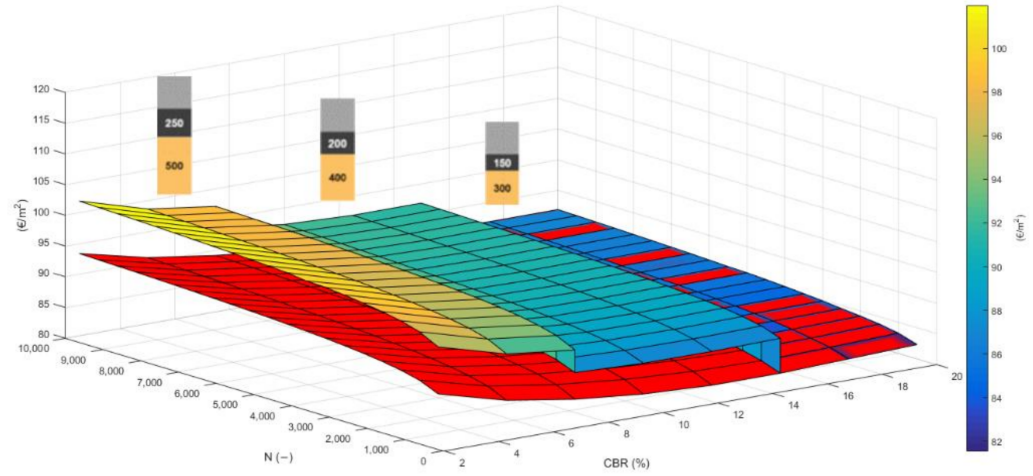

Figure 11. Construction costs with an owned slip form.

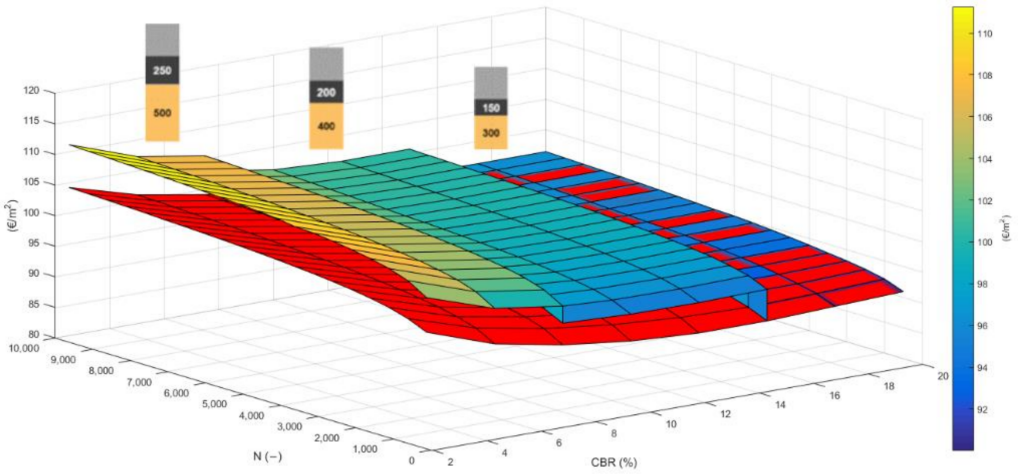

Figure 12. Construction costs with a rented slip form.

In all the designed structures, pavements with 30 cm-thick mixed subbase and 15 cm-thick cement treated base layer are cheaper than those with variable thickness of the bottom layers. Another benefit of the "fixed foundation" is the speed of execution because the laying of thinner layers is faster and easier. In regard to the construction methodology, the use of an owned slip form paver turns out to be cheaper (Figure 13: green surface for laying with a rented slip form, red surface for manual laying, and blue surface for an owned slip form).

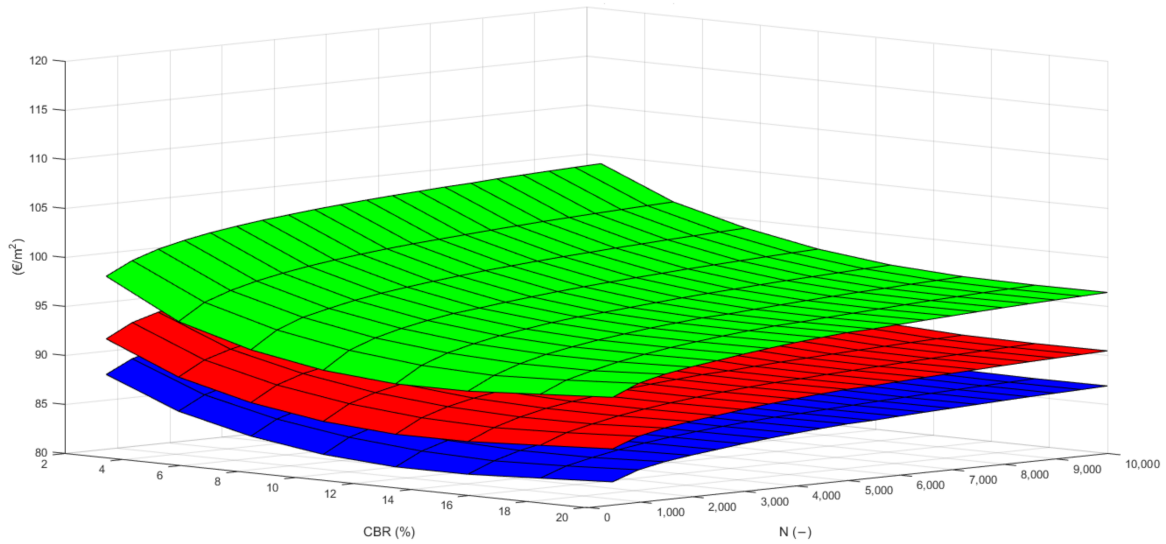

Figure 13. Construction costs for different laying methodologies; scenario 1.

Table 11 lists the construction costs calculated for pavements of scenario 1: they refer to the pavement structures listed in Table 9.

Figure 13 and Table 11 show that using an owned slipform (blue surface) ensures the lower construction costs than manual (red surface) or mechanical laying with a rented slipform (green surface). However, the pavement manager should consider a more complex asset allocation in order to decide on this long-term investment considering its internal rate of return [47].

Table 11. Construction costs vs. slab thickness; scenario 1.

Slab Thickness (cm)	Construction Cost (EUR/m^2)		
	Rented Slipform	Owned Slipform	Fixed Form
29	92.08	83.27	86.68
30	93.92	84.79	88.28
31	95.76	86.32	89.88
32	97.59	87.85	91.48
33	99.41	89.38	93.08
34	101.25	90.90	94.67
35	103.08	92.43	96.27
36	104.92	93.96	97.87

Figure 14a and Figure 14b show the construction costs depending on the number of repetitions when CBR is equal to 2.5% and on the CBR value when *N* is equal to 5000, respectively. Their colors comply with those of Figure 13 (i.e., green for laying with a rented slipform, red for manual laying, and blue for laying with an owned slipform).

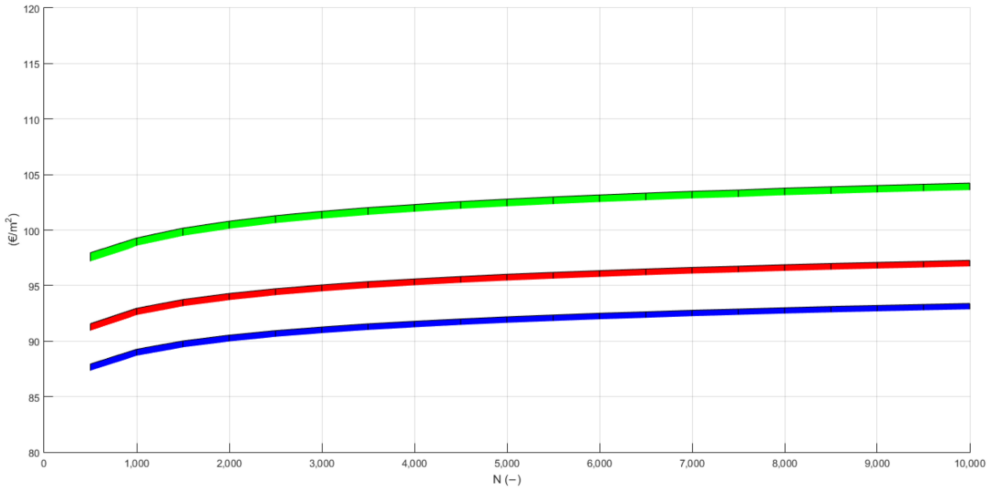

(**a**)

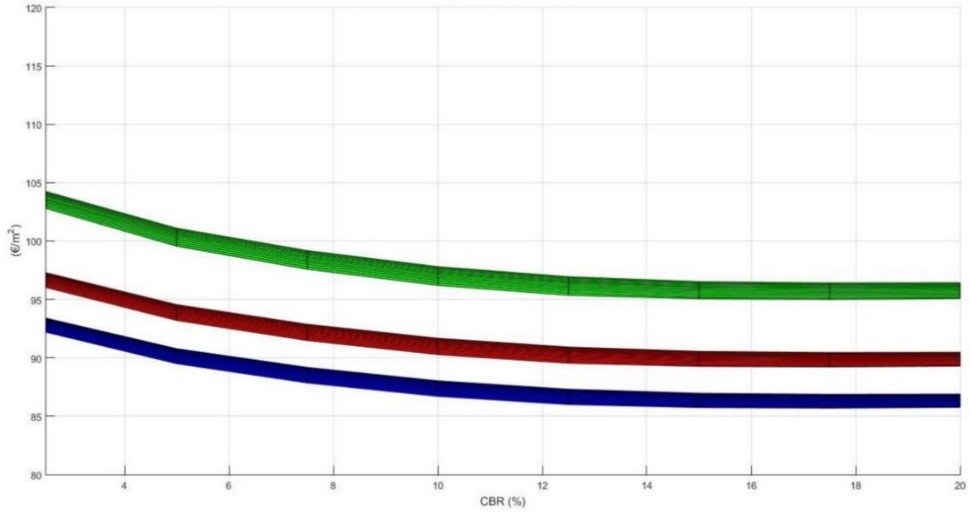

(**b**)

Figure 14. Construction cost curves for scenario 1. (**a**) CBR equal to 2.5%; (**b**) *N* equal to 5000.

Finally, the construction costs for scenario 2 (variable thickness of the bottom layer) were compared. Table 12 lists the results: given a slab thickness value, each cost refers to all the pairs of CBR and *N* in Table 10.

Table 12. Construction costs vs. slab thickness; scenario 2.

Slab Thickness (cm)	Thickness of Bottom Layers—Subbase + Base (cm)	Construction Cost (EUR/m^2)		
		Rented Slipform	Owned Slipform	Fixed Form
24	25 + 50	99.27	91.97	95.03
25		101.09	93.50	96.63
26		102.94	95.02	98.23
27		104.76	96.55	99.83
28		106.60	98.08	101.42
29		108.42	99.61	103.02
30		110.26	101.13	104.62
31		112.10	102.66	106.22
27	20 + 40	96.57	88.36	91.64
28		98.41	89.89	93.23
29		100.23	91.42	94.83
30		102.07	92.94	96.43
31		103.91	94.47	98.03
29	15 + 30	92.08	83.27	86.68
30		93.92	84.79	88.28
31		95.76	86.32	89.88
32		97.59	87.85	91.48

In regard to the economic questions, input data refer to Italian unit prices, but the relative percentage differences between the examined solutions could give preliminary answers to non-Italian airport pavement managers.

4. Discussion

The results of the study are useful to draw up a technical–economic feasibility study [48,49] for a new airport JPCP. Given the design traffic mix and the characteristics of the aircraft that will operate in the 20-year service life, it is possible for each *i*-th airplane to derive the number *N* of take-offs equivalent to the design of the aircraft (i.e., C-130J in this study), using Equation (4):

$$TC_{EQi} = \left(TC_i \; 0.8^{(M-N_i)}\right)^{\sqrt{\frac{W_i}{W}}} \tag{4}$$

where TC_{EQi} is the number of take-offs of the *i*-th airplane equivalent to those of the design airplane; TC_i is the number of take-offs of the *i*-th airplane; *M* is the number of wheels on each leg of the main landing gear of the airplane design; N_i is the number of wheels on each leg of the main landing gear of the *i*-th airplane; *W* is the maximum weight on the single wheel on each leg of the main landing gear of the airplane design; W_i is the maximum weight on the single wheel on each leg of the main landing gear of the *i*-th airplane.

Once the equivalent number of take-offs for each individual aircraft has been calculated, it is possible to obtain the equivalent number of take-offs *N* which permits identification of one of the twenty traffic levels provided in the proposed catalogue (Equation (5)).

$$N = \sum_i TC_{EQi} = \sum_i \left(\left(TC_i \; 0.8^{(M-N_i)}\right)^{\sqrt{\frac{W_i}{W}}} \right) \tag{5}$$

Therefore, the obtained results can be implemented in feasibility studies to solve structural and economic issues regarding an airport JPCP, as currently happens for road pavements [50].

Finally, the findings of this study could be useful for the evaluation of existing airfield pavements that satisfy one of the proposed solutions. Indeed, the proposed catalogue can be used to evaluate the residual life of an old pavement. Given the pavement structure and the subgrade CBR, the number of repetitions of C130J is obtained. If the traffic volume on the pavement in the past is known, it could be evaluated in terms of number of take-offs of C-130J according to Equation 4, and the residual traffic can be estimated. This approach is valid even when the existing structure is not listed in the catalogue: the interpolation between the provided solutions allows estimation of the traffic. On the other hand, as already mentioned, the catalogue can be used only in feasibility studies and for a quick evaluation of the pavement. In the final design phases, traffic must be estimated with a more rigorous calculation method.

5. Conclusions

Most of the Italian military airports derive their structures from concrete pavements built in the post-War period. These structures have been designed, laid and managed all over the State, under different conditions of subgrade bearing capacity, mechanical characteristics of materials, traffic mix, traffic volume during the service life. However, a practical design tool for jointed plain concrete pavements without tie and dowel bars is lacking.

On that basis, the paper presents a catalogue for airport JPCP composed of concrete slabs laid on a cement-treated base and a stabilized granular subbase designed with the software FAARFIELD 1.42 and verified according to the Westergaard theory. All data input about materials and traffic comply with the experience gained by the Italian Air Force. Seven load bearing capacity values (i.e., CBR between 2.5% and 20%), twenty traffic levels (i.e., number of repetitions during the service life between 500 and 10,000), and two scenarios (i.e., constant or variable thickness of the two subbase layers) are examined in the first part of the study to design 170 pavements. The construction costs of each solution are calculated according to the Italian price lists and compared considering three methodologies to pave the concrete slabs (i.e., using a rent slipform paver, using an owned slipform paver, or fixed form). Whatever the methodology adopted to lay the concrete slabs, the construction costs of the first scenario are less than those of the second scenario (e.g., for CBR = 2.5% and N = 500 the construction costs are: 99.41 EUR/m^2, 93.08 EUR/m^2, and 89.38 EUR/m^2 for a rented slipform, fixed form, and an owned form in the first scenario; 104.76 EUR/m^2, 99.83 EUR/m^2, and 96.55 EUR/m^2 for a rented slipform, fixed form, and an owned form in the second scenario).

The results are valid for a single aircraft (i.e., turboprop C-130J), but it is possible to adapt them to a different and non-homogeneous traffic mix. Therefore, both the structural and economic results are interesting and useful, since they provide an inexpensive guide for the preliminary design of JPCP to be laid in airports. Indeed, the proposed catalogue could be used under different conditions because it can be used with different input data (i.e., subgrade bearing capacity, airplane design, traffic mix, construction procedures). The proposed solution could be a valid instrument for design in feasibility studies, when the airport pavement manager should compare different strategies and identify the best option.

Author Contributions: Conceptualization, P.D.M. and A.D.R.; data curation, C.D.M. and G.M.; formal analysis, R.S.; investigation, A.G. and R.S.; methodology, P.D.M.; Software, C.D.M., A.G. and G.M.; supervision, P.D.M., A.D.R. and L.M.; validation, L.M.; visualization, R.S. and L.M.; writing—original draft, L.M.; writing—review and editing, L.M. All authors have read and agreed to the published version of the manuscript.

Funding: This research received no external funding.

Institutional Review Board Statement: Not applicable.

Informed Consent Statement: Not applicable.

Data Availability Statement: All data is contained within the article.

Conflicts of Interest: The authors declare no conflict of interest.

References

1. Hassani, A.; Taghipoor, M.; Karimi, M.M. A state of the art of semi-flexible pavements: Introduction, design, and performance. *Constr. Build. Mater.* **2020**, *253*, 119196. [CrossRef]
2. Breihan, J.R. Review essay: Airport history. *J. Urban Hist.* **2008**, *34*, 850–854. [CrossRef]
3. Sale, J.P.; Hutchinson, R.L. Development of rigid pavement design criteria for military airfields. *J. Air Transp. Div.* **1959**, *85*, 129–151. [CrossRef]
4. Bonin, G.; Cantisani, G.; Loprencipe, G.; Ranzo, A. Dynamic effects in concrete airport pavement joints. [Effetti dinamici nei giunti delle pavimentazioni aeroportuali in calcestruzzo]. *Ind. Ital. Cem.* **2007**, *77*, 590–607.
5. White, G. State of the art: Asphalt for airport pavement surfacing. *Int. J. Pavement Res. Technol.* **2018**, *11*, 77–98. [CrossRef]
6. Moretti, L. Technical and economic sustainability of concrete pavements. *Mod. Appl. Sci.* **2014**, *8*, 1–9. [CrossRef]
7. Loprencipe, G.; Zoccali, P. Comparison of methods for evaluating airport pavement roughness. *Int. J. Pavement Eng.* **2017**, *20*, 782–791. [CrossRef]
8. Loprencipe, G.; Cantisani, G. Evaluation methods for improving surface geometry of concrete floors: A case study. *Case Stud. Struct. Eng.* **2015**, *4*, 14–25. [CrossRef]
9. Orlando, L.; Cardarelli, E.; Cercato, M.; De Donno, G.; Di Giambattista, L. Pavement testing by integrated geophysical methods: Feasibility, resolution and diagnostic potential. *J. Appl. Geophys.* **2017**, *136*, 462–473. [CrossRef]
10. Fan, Z.; Li, C.; Chen, Y.; Di Mascio, P.; Chen, X.; Zhu, G.; Loprencipe, G. Ensemble of deep convolutional neural networks for automatic pavement crack detection and measurement. *Coatings* **2020**, *10*, 152. [CrossRef]
11. Fan, Z.; Li, C.; Chen, Y.; Wei, J.; Loprencipe, G.; Chen, X.; Di Mascio, P. Automatic crack detection on road pavements using encoder-decoder architecture. *Materials* **2020**, *13*, 2960. [CrossRef]
12. Di Mascio, P.; Moretti, L. Implementation of a pavement management system for maintenance and rehabilitation of airport surfaces. *Case Stud. Constr. Mater.* **2019**, *11*, e00251. [CrossRef]
13. Leonelli, F.; Di Mascio, P.; Germinario, A.; Picarella, F.; Moretti, L.; Cassata, M.; De Rubeis, A. Laboratory and on-site tests for rapid runway repair. *Appl. Sci.* **2017**, *7*, 1192. [CrossRef]
14. Corazza, M.V.; D'Alessandro, D.; Di Mascio, P.; Moretti, L. Methodology and evidence from a case study in Rome to increase pedestrian safety along home-to-school routes. *J. Traffic Transp. Eng.* **2020**, *7*, 715–727. [CrossRef]
15. Corazza, M.V.; Di Mascio, P.; Moretti, L. Management of sidewalk maintenance to improve walking comfort for senior citizens. *Urban Transp. XXIII* **2017**, *176*, 195–206. [CrossRef]
16. Di Mascio, P.; Loprencipe, G.; Moretti, L.; Corazza, M.V.; Vivaldi, S.; Vincenti, G. Design of the first Italian roundabout with jointed plain concrete pavement. *Appl. Sci.* **2018**, *8*, 283. [CrossRef]
17. Pleșcan, C.; Pleșcan, E.-L.; Stanciu, M.D.; Botiș, M.; Taus, D. Sensitivity analysis of rigid pavement design based on semi-empirical methods: Romanian case study. *Symmetry* **2021**, *13*, 168. [CrossRef]
18. Federal Aviation Administration. *AC 150/5320-6F—Airport Pavement Design and Evaluation*; Federal Aviation Administration: Washington, DC, USA, 2016.
19. Daggubati, S.C.; Nazneen; Sharma, S.; Raj, S. Runway design and structural design of an airfield pavement. *IOSR J. Mech. Civ. Eng.* **2014**, *11*, 10–27. [CrossRef]
20. Westergaard, H.M. Stresses in concrete pavements computed by theoretical analysis. *Public Roads* **1926**, *7*, 25–35.
21. Bonucci, P.T.; Lu, J.W.Z.; Leung, A.Y.T.; Iu, V.P.; Mok, K.M. Airfield rigid pavement structural design—A review of main aspects and methods of analysis. In Proceedings of the AIP Conference Proceedings, Hong Kong, Macau, China, 30 November–3 December 2009; AIP Publishing: Melville, NY, USA, 2010; Volume 1233, p. 1339.
22. NATO (North Atlantic Treaty Organization). *NATO Approved Criteria and Standards for Airfields—BI-SC DIRECTIVE 85-5*; North Atlantic Treaty Organization: Brussels, Belgium, 2010.
23. AASHTO. *AASHTO Guide for Design of Pavement Structures*; American Association of State Highway and Transportation Officials: Washington, DC, USA, 1993.
24. EN (European Committee for Standardization). *EN 933-2:2020—Tests for Geometrical Properties of Aggregates, Part 2: Determination of Particle Size Distribution, Test Sieves, Nominal Size of Apertures*; European Committee for Standardization: Brussels, Belgium, 2020.
25. EN (European Committee for Standardization). *EN 933-5:2004—Tests for Geometrical Properties of Aggregates, Part 5: Determination of Percentage of Crushed and Broken Surfaces in Coarse Aggregate Particles*; European Committee for Standardization: Brussels, Belgium, 2004.
26. EN (European Committee for Standardization). *EN 1097-2:2010—Tests for Mechanical and Physical Properties of Aggregates, Part 2: Methods for the Determination of Resistance to Fragmentation*; European Committee for Standardization: Brussels, Belgium, 2020.
27. EN (European Committee for Standardization). *EN 933-4:2008—Tests for Geometrical Properties of Aggregates, Part 4: Determination of Particle Shape Index*; European Committee for Standardization: Brussels, Belgium, 2008.

28. EN (European Committee for Standardization). *EN 933-3:2012—Tests for Geometrical Properties of Aggregates, Part 3: Determination of Particle Shape Flakiness Index*; European Committee for Standardization: Brussels, Belgium, 2012.
29. EN (European Committee for Standardization). *EN 1367-1:2007—Tests for Thermal and Weathering Properties of Aggregates, Part 1: Determination of Resistance to Freezing and Thawing*; European Committee for Standardization: Brussels, Belgium, 2007.
30. EN (European Committee for Standardization). *EN 933-1:2012—Tests for Geometrical Properties of Aggregates, Part 1: Determination of Particle Size Distribution Sieving Method*; European Committee for Standardization: Brussels, Belgium, 2012.
31. EN (European Committee for Standardization). *EN ISO 17892-12:2018—Geotechnical Investigation and Testing Laboratory Testing of Soil, Part 12: Determination of Liquid and Plastic Limits (ISO 17892-12:2018)*; European Committee for Standardization: Brussels, Belgium, 2018.
32. EN (European Committee for Standardization). *EN 933-8:2015—Tests for Geometrical Properties of Aggregates, Part 8: Assessment of Fines Sand Equivalent Test*; European Committee for Standardization: Brussels, Belgium, 2015.
33. ASTM (American Society for Testing and Materials International). *ASTM D1883-16—Standard Test Method for California Bearing Ratio (CBR) of Laboratory-Compacted Soils*; ASTM International: West Conshohocken, PA, USA, 2016.
34. EN (European Committee for Standardization). *EN 197-1:2000—Cement Part 1: Composition, Specifications and Conformity Criteria for Common Cements*; European Committee for Standardization: Brussels, Belgium, 2000.
35. EN (European Committee for Standardization). *EN 1008:2002—Mixing Water For Concrete, Specification for Sampling, Testing and Assessing the Suitability of Water, Including Water Recovered From Processes in the Concrete Industry, as Mixing Water for Concrete*; European Committee for Standardization: Brussels, Belgium, 2002.
36. EN (European Committee for Standardization). *EN 12390-3:2019—Testing Hardened Concrete, Part 3: Compressive Strength of Test Specimens*; European Committee for Standardization: Brussels, Belgium, 2019.
37. EN (European Committee for Standardization). *EN 12390-6:2009. Testing Hardened Concrete, Part 6: Tensile Splitting Strength of Test Specimens*; European Committee for Standardization: Brussels, Belgium, 2009.
38. Federal Aviation Administration. *AC 150/5370-10G—Standards for Specifying Construction of Airports*; Federal Aviation Administration: Washington, DC, USA, 2014.
39. EN (European Committee for Standardization). *EN 12390-5:2019—Testing Hardened Concrete, Part 5: Flexural Strength of Test Specimens*; European Committee for Standardization: Brussels, Belgium, 2019.
40. EN (European Committee for Standardization). *EN 206:2013+A1:2016—Concrete, Specification, Performance, Production and Conformity*; European Committee for Standardization: Brussels, Belgium, 2016.
41. Di Mascio, P.; Loprencipe, G.; Moretti, L. Technical and economic criteria to select pavement surfaces of port handling plants. *Coatings* **2019**, *9*, 126. [CrossRef]
42. ANAS. Listino Prezzi Nuove Costruzioni e Manutenzione Straordinaria. Available online: https://www.stradeanas.it/sites/default/files/NC-MS_LISTINO%20PREZZI%202021.pdf (accessed on 28 March 2021).
43. Regione Lazio. Lavori Stradali e Infrastrutture a Rete. Available online: http://www.regione.lazio.it/binary/rl_main/tbl_documenti/INF_DGR_955_04_12_2020_Allegato_4.pdf (accessed on 28 March 2021).
44. Regione Sardegna. Prezziario Opera Pubbliche Regione Sardegna. 2018. Available online: http://www.regione.lazio.it/rl_infrastrutture/?vw=contenutiDettaglio&cat=1&id=122 (accessed on 28 March 2021).
45. Moretti, L.; Di Mascio, P.; Panunzi, F. Economic sustainability of concrete pavements. *Procedia Soc. Behav. Sci.* **2012**, *53*, 125–133. [CrossRef]
46. Packard, R.G. *Design of Concrete Airport Pavement*; Portland Cement Association: Skokie, IL, USA, 1973.
47. Haas, R.; Tighe, S.; Falls, L.C. Determining return on long-life pavement investments. *Transp. Res. Rec. J. Transp. Res. Board* **2006**, *1974*, 10–17. [CrossRef]
48. Miccoli, S.; Finucci, F.; Murro, R. Assessing project quality: A multidimensional approach. *Adv. Mater. Res.* **2014**, *1030–1032*, 2519–2522. [CrossRef]
49. Miccoli, S.; Finucci, F.; Murro, R. A new generation of urban areas: Feasibility elements. In Proceedings of the Advances in Energy Equipment Science and Engineering, Guangzhou, China, 30–31 May 2015; Apple Academic Press: Palm Bay, FL, USA, 2015; Volume 2, pp. 1445–1449.
50. Di Mascio, P.; Moretti, L.; Capannolo, A. Concrete block pavements in urban and local roads: Analysis of stress-strain condition and proposal for a catalogue. *J. Traffic Transp. Eng.* **2019**, *6*, 557–566. [CrossRef]